Hindawi
Advances in Civil Engineering
Volume 2019, Article ID 2183732, 12 pages
https://doi.org/10.1155/2019/2183732

Research Article

Stability Analysis of Slope with Multiple Sliding Surfaces Based on Dynamic Strength-Reduction DDA Method

Shuhong Wang, Chengjin Zhu, Pengyu Wang, and Zishan Zhang

School of Resources and Civil Engineering, Northeastern University, Shenyang 110819, China

Correspondence should be addressed to Chengjin Zhu; zhuchengjin@cumt.edu.cn

Received 15 July 2019; Revised 23 September 2019; Accepted 1 October 2019; Published 11 November 2019

Academic Editor: Yinshan Tang

The present study aims to elucidate the problem of a rock mass structural plane with a range of damage degrees and the numerical model selection for analysis of a slope with multiple sliding surfaces. Based on the relative displacement between blocks, the dynamic strength reduction-discontinuous deformation analysis (hereinafter referred to as DSR-DDA) method is proposed for studying slopes with multiple sliding surfaces. The slope-slider classic case was used to test the displacement threshold. The model was applied to the stability analysis of multiple sliding surfaces of a high rock slope in the Fushun West Open-Pit Mine. The results show that when the displacement threshold is set to 1 mm, the error between the DSR-DDA results and the theoretical solution is within 0.5%, which satisfies the calculation requirements. The most dangerous slip surface in the Fushun West Open-Pit Mine slope was identified. Based on the numerical slope model after the first landslide, the position of the secondary slip surface was then identified. The failure mode is traction sliding failure, and the middle and lower oil shales play a key role in the slope stability. This study recommends that mining of the remaining oil shale should stop to avoid causing large-scale landslides in the upper part of the slope and landslides at the pit-city boundary.

1. Introduction

Large-scale geographical areas have complicated geological and instability conditions. A high slope with an open pit forms large areas prone to secondary instability after initial instability, resulting in a secondary sliding surface. The high rock slope is affected by the bedding structure, which complicates the stability problem of the slope. Therefore, it is necessary to elucidate the stability of rock high slopes with multiple potential sliding surfaces through research [1–8].

There are two commonly used calculation methods in slope stability analysis: the limit equilibrium method (LEM) [9–11] and finite element method (FEM) [12–14]. Compared with the FEM, the LEM has a high computational efficiency. The safety factor is solved by geometric assumptions based on known or assumed slip surfaces, but the constitutive relationship of rock and soil during slope slip is ignored [15]. In recent years, with the rapid development of FEMs and the combination of strength reduction methods, models no longer need to presuppose the position of the sliding surface. The safety factor and corresponding potential sliding surface are easy to obtain. The limitation lies in the safety factor and singularity of the sliding surface solution. Cala et al. [16] pioneered a new strength-reduction method, which identified the most dangerous instability surface based on the conventional method. The authors determined the number of steps N for the first slip and continued to increase the reduction factor; then, the results of the 1.1 N step were calculated. The corresponding secondary potential instability surface and safety factor were successively obtained. However, there is a need to further study these methods for the stability analysis of slopes with multiple sliding surfaces.

Discontinuity is an intrinsic property of a rock mass. The discontinuous deformation analysis (DDA) proposed by Shi [17] has unique advantages in simulating

large block displacement and large deformation. DDA has also been rapidly developed in the field of slope engineering. Maclaughlin et al. [18] simulated the plane and arc failure modes of inclined slopes and found that the results had better accuracy than those of the conventional analysis methods. Hatzor and Feintuch [19] showed the validity of DDA results for the full dynamic analysis of dynamically charged monolithic slopes. Beyabanaki [20] presented existing blocks in discontinuity failure analysis as deformable disks. Jiang and Zheng [21] proposed an effective method to correct the error in the increase in volume caused by a large rotation. Morgan and Aral [22] proposed a hydrogeological model to model hydraulic breaks using deformed breakdown analysis. This model complies with the Griffith model. The elasticity problem of a large rotation has been previously studied [23]. Perturbations occur in the initial DDA because the first-order shift function is used to describe the block's movement. Yu and Yin [24] have improved some algorithms and processes used to analyze the deformation of discontinuities. Biran and Hatzor [25] compared the DDA with a powerful discrete structure and component numerical modeling method. Zheng et al. [26] used the dual form of this method to solve the problem of opening and closing iterations and strong applied forces. Fu et al. [27] combined the border element method with the DDA to achieve synchronous deformation modeling and displacement modeling. Fan et al. [28, 29] used virtual work theory to improve the accuracy of deformation and large rotation error estimation and proposed a new method to identify and analyze the contact blocks. Fu et al. [30] applied the vector sum method (VSM) to the DDA to calculate the slope stability safety factor based on the actual stress state and vector and algorithm. There is a lack of studies regarding the stability analysis of a slope with multiple sliding surfaces using these methods.

Shahami et al. [31] studied the effects of external loading changes on the rock block displacements in the DDA method. The results show that the effects of external forces on the stability of the blocky rock mass depend on the magnitude of the applied forces and the dimensions of the blocks that constitute the rock mass. Gong et al. [32] proposed the improved DDA (IDDA) method, which could more effectively provide a unified formulation to simulate the nonlinear deformation and failure behaviors of jointed rock masses. Chen et al. [33] clarified the postfailure behavior of a landslide using a two-dimensional (2D) DDA and provided comprehensive information on the initiation and evolution of the landslide. Fan et al. [34] introduced a partitioned finite element and interface element (PFE/IE) interactive method and analyzed the dynamic behaviors of structures with discontinuous deformations. Moreover, PFE/IE improves the computational efficiency because the nonlinear iteration is limited to the possible contact region. Liu et al. [35] extended the flat-top partition of the unity method that could obtain a stiffness matrix with a small condition number and avoid the linear dependence problem to rock dynamic analyses to simulate the effect of the discontinuity and dynamic loading.

The key problem in the development of slope stability evaluation is the safety factor and solution of the corresponding slip surface. Previously, the strength reduction method mostly assumes a uniform reduction in a rock mass. In an actual situation, the mechanical properties of the structural plane mainly determine the mechanical properties of the rock mass. However, the structural damage of a rock mass does not exhibit the same degree of damage through time. After the first instability of the slope, the block position and stress redistribute. Therefore, the secondary slip surface should be analyzed using the slope model after the first instability. In the past, the secondary sliding surface of the slope was studied. Few studies have considered the actual situation. To solve this problem, we draw on the advantage of DDA to calculate the displacement and consider the relative displacement between blocks. We proposed a multiple-sliding-surface search based on the DSR-DDA method and evaluated the slope stability. This method is mainly applied to solve rock mass stability problems, especially for large-scale rock masses with numerous structural planes. Moreover, this method can consider the variation in damage along a rock mass structural plane and help with numerical model selection in the analysis of a slope with multiple sliding surfaces. By analyzing a rock mass using this method, we can easily determine the safety factor and corresponding slip surface. Thus, measures can be taken to prevent the instability of a rock mass over time. We used an inclined plane slider to test the displacement threshold and verify the feasibility and accuracy of the proposed method and attempted to apply this approach to the stability analysis of a rock high slope in the Fushun West Open-Pit Mine.

2. Methodology

2.1. Main Features of the DDA. The DDA uses a first-order displacement function to express the motion parameters of each block and assumes that the stress and strain are cconstant [36]. The displacement vector of each block contains 6 variables as follows:

$$D = \left(u_0, v_0, r_0, \varepsilon_x, \varepsilon_y, \gamma_{xy}\right)^{\mathrm{T}}, \tag{1}$$

where (u_0, v_0) is the rigid displacement of a specific point (x_0, y_0) in the block; r_0 is the rotation angle of the block around a specific point (x_0, y_0); and $\varepsilon_x, \varepsilon_y, \gamma_{xy}$ is the positive strain and the shear strain of the block, respectively. The displacement (u, v) of any point (x, y) in the block is as follows:

$$\begin{Bmatrix} u \\ v \end{Bmatrix} = [T]\{D\} = \begin{bmatrix} 1 & 0 & -(y-y_0) & (x-x_0) & 0 & (y-y_0)/2 \\ 0 & 1 & (x-x_0) & 0 & (y-y_0) & (x-x_0)/2 \end{bmatrix} \cdot \begin{Bmatrix} u_0 \\ v_0 \\ r_0 \\ \varepsilon_x \\ \varepsilon_y \\ \gamma_{xy} \end{Bmatrix}. \tag{2}$$

The overall equilibrium equation of the system based on the principle of minimum potential energy is as follows:

$$\begin{bmatrix} K_{11} & K_{12} & \cdots & K_{1n} \\ K_{21} & K_{22} & \cdots & K_{2n} \\ \cdots & \cdots & \ddots & \cdots \\ K_{n1} & K_{n2} & \cdots & K_{nn} \end{bmatrix} \begin{Bmatrix} D_1 \\ D_2 \\ \vdots \\ D_n \end{Bmatrix} = \begin{Bmatrix} F_1 \\ F_2 \\ \vdots \\ F_n \end{Bmatrix}, \tag{3}$$

where K_{ij} is a 6×6 submatrix in the coefficient matrix; K_{ii} is determined by the material properties and geometric parameters of the block unit; $K_{ij}\,(i \neq j)$ is determined by the contact conditions between block i and block j; $[D_i]$ and $[F_i]$ are 6×1 submatrices; D_i is the deformation variable $(d_{1i}, d_{2i}, d_{3i}, d_{4i}, d_{5i}, d_{6i})$ block i; and F_i is the load assigned to the six deformation variables on block i.

2.2. DSR-DDA Method Displacement Threshold. To consider the dissimilarity of the damage along the block structure surface in the real situation, it is proposed that the shear strength of the block structure surface is reduced so that the displacement change does not exceed the threshold value. We used the classic slope slider case to test the displacement threshold of the shear strength reduction. The model is shown in Figure 1. The rock mass parameters are shown in Table 1. In the program calculation, the shear strength parameters of the structural plane of the block are set at regular intervals (10,000 steps, each time step is 0.001 s). According to the relationship between the relative displacement change in the block and the threshold value, only the structural plane with the displacement change that satisfies the requirements was selected. Then, the reduction increases by 0.001 from 1.000 until a sharp deformation occurs, at which time the value of the safety factor of the slope slip surface is determined. The program calculates the simulated reduction process that is consistent with the damage degradation of the rock mass material under actual conditions.

The theoretical safety factor of the simple slope model is as follows:

$$F_s = \frac{\tan \varphi}{\tan \alpha}. \tag{4}$$

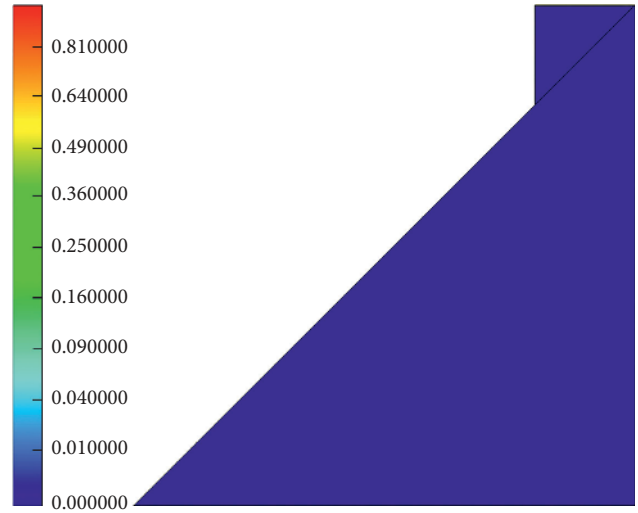

Figure 1: Model of the sliding block along the slope.

Figure 2 shows the variation in the model safety factor and error percentage of the analytical solution with the displacement threshold under different values of the in-plane friction angle φ. This graph shows that, regardless of the value of the internal friction angle φ, when the displacement threshold approaches 1 mm, the safety factor is near its maximum value. There is a significant dip in the error percentage of the analytical solution, which indicates that the error is relatively small, within 0.5%. The displacement threshold is temporarily taken as 1 mm. The results of the analytical solution are consistent. Hence, the DSR-DDA method satisfies the calculation requirements and can guarantee a certain calculation accuracy.

Finding the exact solution of the contact force between the blocks is the core step in solving the total equilibrium equation. In each time step, it is necessary to redetermine the application of the spring and position of the spring. It is necessary to repeatedly generate a solution to solve the total stiffness matrix. The process of application and removal of the rigid spring is called an open-close iteration. There are three states of contact: opening, sliding, and locking. The criteria to determine the mode change are shown in Table 2.

Based on the above analysis, the DSR-DDA method is implemented in the program as shown in Figure 3.

3. Rock Slope Model and Parameters of Fushun Western Open-Pit Mine

3.1. Overview of the Rock Slope in Fushun Western Open-Pit Mine. The Fushun West Open-Pit Mine is located in the southeastern part of Fushun City and has a mining history of more than 100 years. It has formed "Asia's largest pit" with a length of 6.6 km, a width of 2.2 km from north to south, and a depth of 400–500 m, representing a total volume of 1.7 billion cubic kilometers. The northern part of the coal-mining pit is adjacent to the urban area of Fushun City. If a landslide occurs in the northern slope, it will cause a large number of casualties and major property loss, seriously affecting the safety of all nearby construction facilities and endangering the safety of

Table 1: Mechanical properties of the slope model.

Number	Density (kg·m^{-3})	E (MPa)	Cohesion (MPa)	Friction (°)	Poisson's ratio	Theoretical safety factor
01	2700	1000	40	50	0.35	1.192
02	2700	1000	40	55	0.35	1.428
03	2700	1000	40	60	0.35	1.732
04	2700	1000	40	65	0.35	2.145
05	2700	1000	40	70	0.35	2.747
06	2700	1000	40	75	0.35	3.732
07	2700	1000	40	80	0.35	5.671

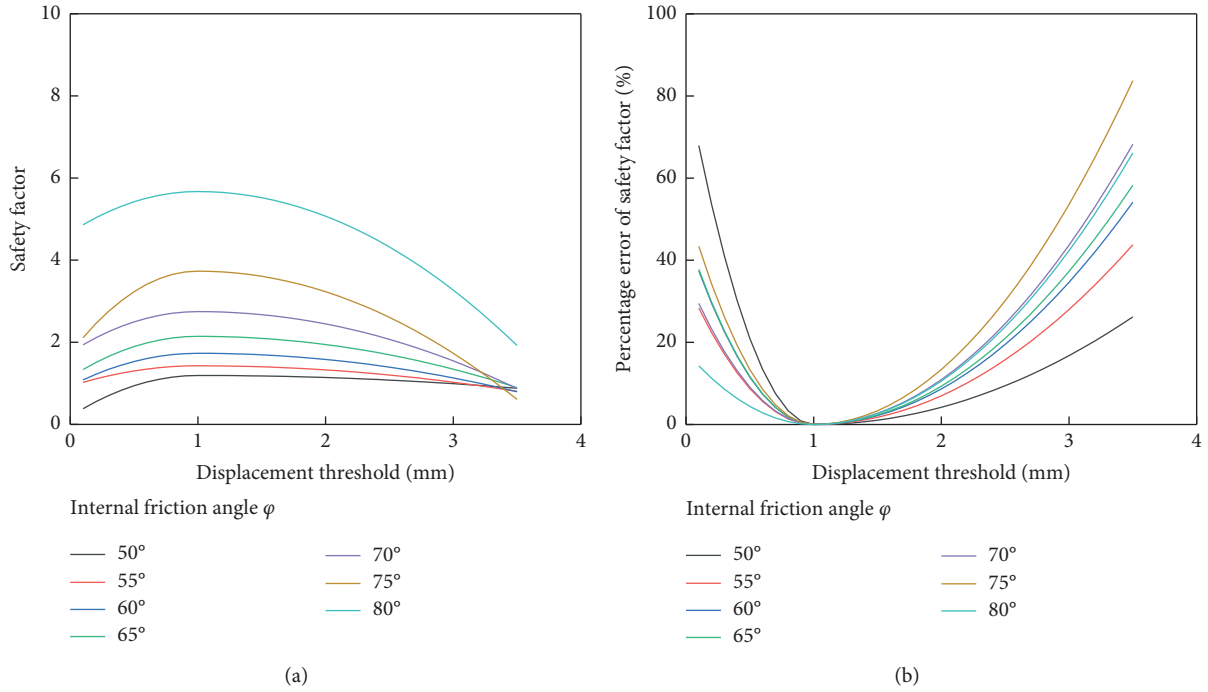

Figure 2: Curve of safety factor and its error with the displacement threshold: (a) safety factor; (b) percentage error of safety factor.

Table 2: Contact status table.

Contact switch	Contact condition	Contact force
Open-open	$\mathbf{N} > 0$	No
Open-sliding	$\mathbf{N} < 0$, $\lvert\mathbf{S}\rvert > \lvert\mathbf{f}\rvert$	Yes
Open-locked	$\mathbf{N} < 0$, $\lvert\mathbf{S}\rvert < \lvert\mathbf{f}\rvert$	Yes
Sliding-open	$\mathbf{N} > 0$	No
Sliding-sliding	$\mathbf{N} < 0$, $\lvert\mathbf{S}\rvert > \lvert\mathbf{f}\rvert$ or $\mathbf{N} < 0$, $\psi = -\text{sgn } \mathbf{f}$	Yes
Sliding-locked	$\mathbf{N} < 0$, $\lvert\mathbf{S}\rvert < \lvert\mathbf{f}\rvert$ or $\mathbf{N} < 0$, $\psi = \text{sgn } \mathbf{f}$	Yes
Locked-open	$\mathbf{N} > 0$	No
Locked-sliding	$\mathbf{N} < 0$, $\lvert\mathbf{S}\rvert > \lvert\mathbf{f}\rvert$	Yes
Locked-locked	$\mathbf{N} < 0$, $\lvert\mathbf{S}\rvert < \lvert\mathbf{f}\rvert$	Yes

[1]$\boldsymbol{N}$ is the normal contact force, $\boldsymbol{S}$ is the shear contact force, ψ is the direction of shear displacement, and f is the frictional force.

the entire city. The layout of the Fushun West Open-Pit Mine and the northern part of the western slope are shown with a geological section map in Figure 4.

3.2. Calculation Analysis Model and Parameters. Discontinuous structures such as joints and fissures play a controlling role in the deformation of a rock mass. The accuracy of the information acquisition of the structural plane is critical to the accuracy of the numerical simulation analysis. Using high-precision and high-efficiency unmanned aerial vehicle technology, deterministic structural plane information is accurately acquired to generate a point cloud model [37]. The DJI Phantom 4 Pro and control system are shown in Figure 5.

The definition of inclination requires that the surface structure of the rock mass is known, including the normal vector of the plane where the production is located, assuming that the equation representing the structural plane is as follows:

$$Z = AX + BY + C, \tag{5}$$

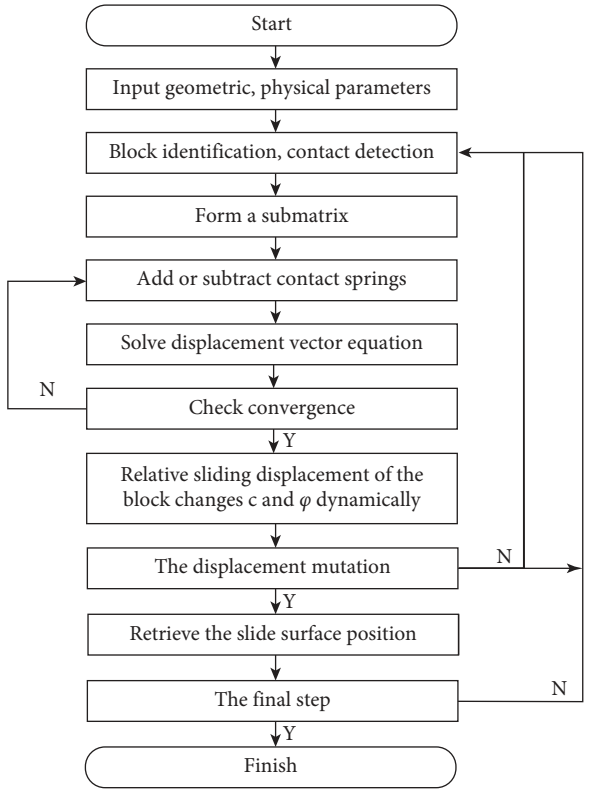

Figure 3: Flow chart of the DDA procedures.

where A, B, and C are plane parameters, and the plane normal vector n is $(-A, -B, 1)$. Along the structural plane, for any n points that are not collinear ($n > 3$), we can obtain the following equation:

$$\begin{bmatrix} X_1 & Y_1 & 1 \\ X_2 & Y_2 & 1 \\ X_3 & Y_3 & 1 \\ \cdots & \cdots & \cdots \\ X_n & Y_n & 1 \end{bmatrix} \cdot \begin{bmatrix} A \\ B \\ C \end{bmatrix} = \begin{bmatrix} Z_1 \\ Z_2 \\ Z_3 \\ \cdots \\ Z_n \end{bmatrix}. \tag{6}$$

The least squares method is used to solve (A, B, C) as follows:

$$\begin{bmatrix} A \\ B \\ C \end{bmatrix} = \left(\begin{bmatrix} X_1 & Y_1 & 1 \\ X_2 & Y_2 & 1 \\ X_3 & Y_3 & 1 \\ \cdots & \cdots & \cdots \\ X_n & Y_n & 1 \end{bmatrix}^{\mathrm{T}} \begin{bmatrix} X_1 & Y_1 & 1 \\ X_2 & Y_2 & 1 \\ X_3 & Y_3 & 1 \\ \cdots & \cdots & \cdots \\ X_n & Y_n & 1 \end{bmatrix} \right)^{-1} \begin{bmatrix} X_1 & Y_1 & 1 \\ X_2 & Y_2 & 1 \\ X_3 & Y_3 & 1 \\ \cdots & \cdots & \cdots \\ X_n & Y_n & 1 \end{bmatrix}^{\mathrm{T}} \begin{bmatrix} Z_1 \\ Z_2 \\ Z_3 \\ \cdots \\ Z_n \end{bmatrix}. \tag{7}$$

From the conversion formula, the dip direction is as follows:

$$\alpha = \arctan\left|\frac{B}{A}\right|. \tag{8}$$

The dip angle is as follows:

$$\beta = \left|\arctan\left(\sqrt{A^2 + B^2}\right)\right|. \tag{9}$$

The point cloud parameters of the structural plane are selected. The plane equation is fitted according to the point cloud information, and the structural surface morphology is determined. The calculation results of some occurrences are shown in Table 3, and the structural plane production statistics are obtained. The statistical cloud chart of the structural plane is shown in Figure 6.

The acquired structural plane information is imported into the DSR-DDA program, and the structural plane mesh cuts the rock mass to form a block unit in the DSR-DDA. Figure 7 shows a model of the example for numerical analysis.

The natural stress field takes only gravity into account and does not include the regional tectonic stress. According to the geological exploration and test results, the parameters in Table 4 are obtained. The cohesion and friction in Table 4 are the implied cohesion and friction values of the rock mass structural plane. In the numerical calculation, the shear strength parameters of the structural plane of the block are reduced at a certain time step (10,000 steps, each time step is approximately 0.001 seconds) along the structural plane where the relative displacement change in the block is reached or exceeded, and the reduction factor changes from 1.000. Initially, this time step is consistent with the damage degradation of the rock mass material.

4. Stability Analysis of the Rock Slope in Fushun Western Open-Pit Mine

4.1. Field Displacement Monitoring. The cumulative displacement values measured at different depths in each inclined hole during two months are shown in Figure 8.

The analysis of Figure 8 shows that the total displacement value of the measured point in the first 100 m of hole 69002 greatly varies with time. The magnitude of displacement sharply increases near a depth of 100 m, which indicates that the rock mass near the inclined hole slips. There is a tendency to continue sliding, and the sliding surface is approximately 100 m from the slope. The total displacement of the measuring point in the first 20 m of hole 55026 occurs relatively fast, and there is a trend of continued growth. The change in displacement at the subsequent measuring point is not obvious and tends to be stable. It is speculated that instability exists in the rock mass above the measuring hole. The displacement of the measuring point in hole 74003 slowly increases with time, with no obvious regularity, and tends to be stable; thus, the stability of the rock mass in this area is better than those at other holes.

4.2. DSR-DDA Numerical Calculation Analysis. To further determine the potential slip surface position of the slope, according to the DSR-DDA method, the shear strength parameters are dynamically reduced, and the progressive instability of the slope was characterized. The slip surface and corresponding safety factor were measured. The feasibility of the method was verified by identifying the most dangerous slip surface and secondary slip surface in the slope. Figures 9 and 10 show the first instability and secondary instability of the slope. The legend in these figures indicates the displacement of the block at the current time step. For example, 0.706876 indicates that the block moves 0.706876 mm in the current time step.

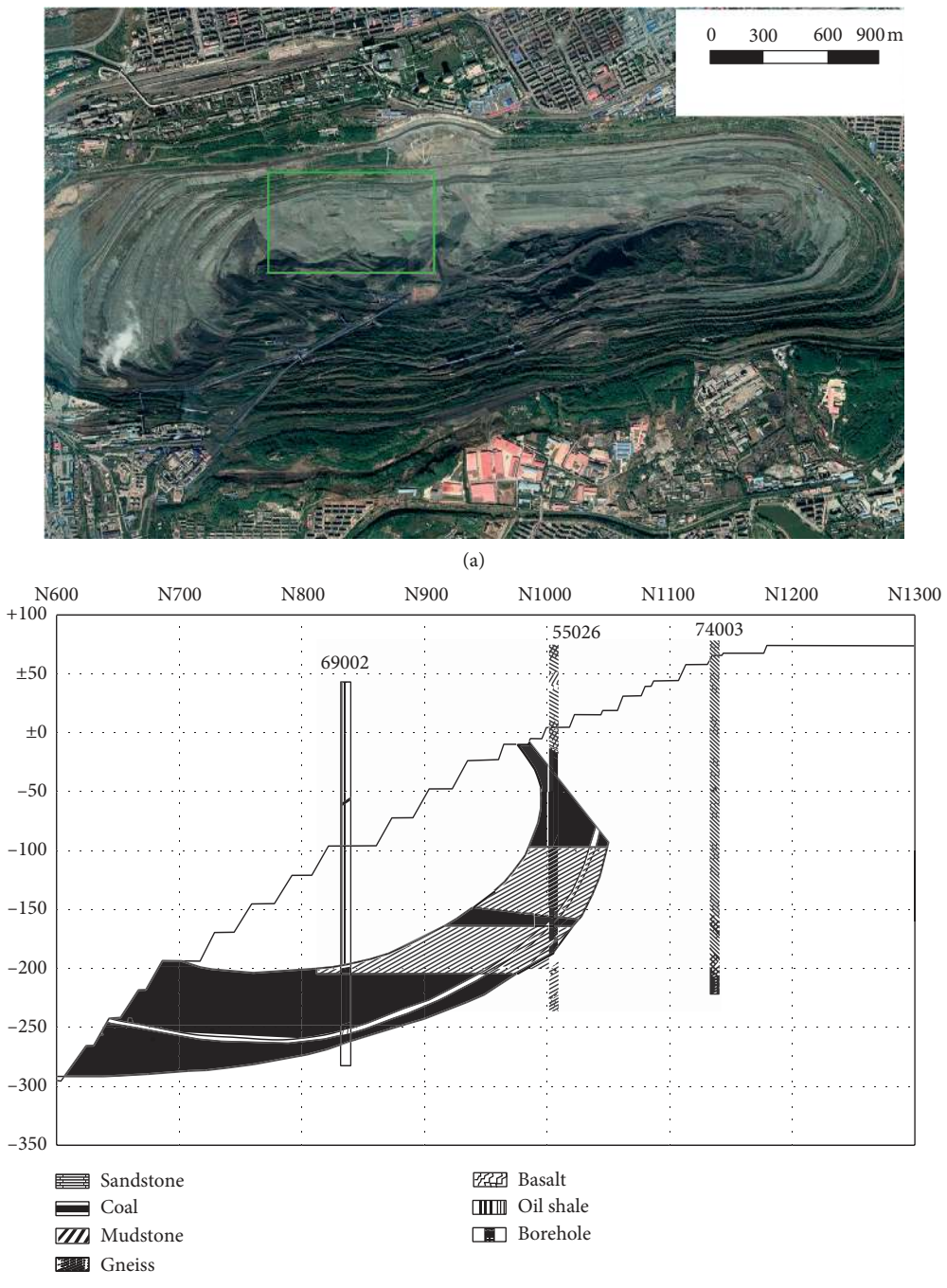

Figure 4: Layout of the Fushun West Open-Pit Mine and the northern part of the western slope in the geological section map: (a) Fushun West Open-Pit Mine; (b) geological section map.

Before the 1.360×10^6 time step, the displacement of the monitoring points of each block and the overall slope of the block remain basically stable. When the calculation is at step 1.360×10^6, the slope quickly deforms, the reduction factor reaches 1.136, and the displacement of the corresponding block sharply increases. The subsequent deformation also shows a gradual increasing trend. The overall deformation of the slope shows that the lower landslide body slips along the corresponding sliding surface, which indicates that the slope is unstable for the first time. The safety factor corresponding to the most dangerous slip surface was 1.136.

According to the block large deformation data and DSR-DDA program image, the slope slip surface appears at a depth of approximately 100 m in hole 69002. The large deformation of the rock mass occurs above the sliding surface. The position of the deep part of hole 55026 does not significantly change, and only the block in the near-surface position is displaced. There is no obvious deformation of the

Figure 5: DJI Phantom 4 Pro and control system.

Table 3: Yield calculation results.

Number	Structural plane equation parameter			Structural plane information		
	A	B	C	Dip direction (°)	Dip angle (°)	The length of the trace (m)
01	0.368	0.245	0.621	33.7	35.5	6.55
02	0.440	−1.270	0.265	109.0	78.9	6.70
03	0.337	2.824	0.324	263.2	83.5	8.53
04	−1.380	3,452	0.443	291.8	83.2	4.26
05	0.455	2.088	0.266	282.3	82.9	2.88
06	−0.100	1.480	0.185	265.9	82.9	1.20
07	−0.640	5.600	0.247	96.6	73.2	5.88
08	0.316	0.882	0.201	250.3	77.9	1.47
09	0.447	1.703	0.247	284.7	89.0	2.06
10	57.150	−28.400	0.433	26.5	89.6	1.95

rock mass in hole 74003. These characteristics are consistent with the on-site monitoring data, which further proves the feasibility of the method.

After the first instability of the slope, the block position and internal stress are redistributed. The slope modeling continued after the first instability process to identify the secondary slip surface.

Before step 1.890×10^6, the slope tends to be stable. When the calculation is completed at step 1.890×10^6, the reduction factor reaches 1.189. The slope again quickly deforms and forms a secondary slip surface. Its corresponding safety factor is 1.189. The slope of the first slope is larger than the first slope instability. The slope strength is slightly reduced after the first instability occurs, which is notably different from the results obtained by the conventional analysis.

The failure mode of the slope of the Fushun West Open-Pit Mine is traction-type sliding failure. The middle and lower oil shales play a key role in the stability of the slope. Therefore, the remaining oil shale cannot be continuously mined to avoid large-scale landslides from initiating in the upper part of the slope and to avoid landslides at the pit-city boundary.

5. Discussion

In this paper, we theoretically confirmed the necessity and significance of dynamically reducing the strengths of rock mass structural planes. We further revealed the effects of the problem of different degrees of damage of rock mass structural planes and the problem of numerical model selection for analyzing slopes with multiple sliding surfaces. We determined the displacement threshold to reduce the error between DSR-DDA and the theoretical solution. Then, we used these methods in the stability analysis of the northern slope of the Fushun West Open-Pit Mine.

In addition, the slope strength is slightly reduced after the first instability occurs, which is quite different from the results obtained by conventional analysis [38, 39]. We infer that the first instability landslide body cannot be ignored in the conventional analysis because it protects the secondary landslide body with a high safety factor, mainly because the position and stress of the block are redistributed after the first instability of the slope. Therefore, the secondary slip surface should be analyzed using the slope model after the first instability, which was not fully considered in previous studies.

Although there are advantages in the DSR-DDA method for slope-stability analysis and large-deformation slope-instability analysis, there are still weaknesses in the precision of the method. It is difficult to complete slope failure experiments in the laboratory. The displacement threshold is set by the DSR-DDA numerical simulation test, which makes the accuracy of the results overly dependent on the accuracy of the DSR-DDA program. Therefore, the results suggest that, in the future, different projects will require simulation training to improve their accuracy and that similar laboratory experiments should be attempted. For further study,

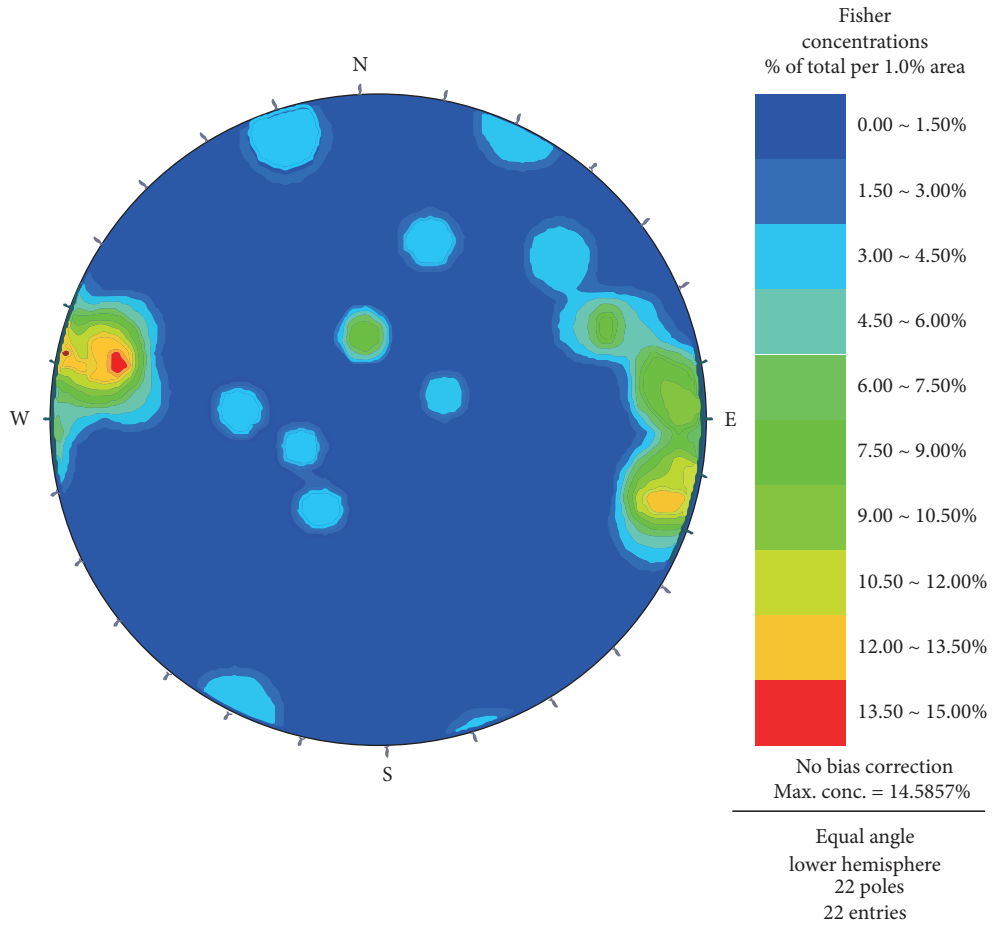

Figure 6: Statistical cloud chart of the structure surface.

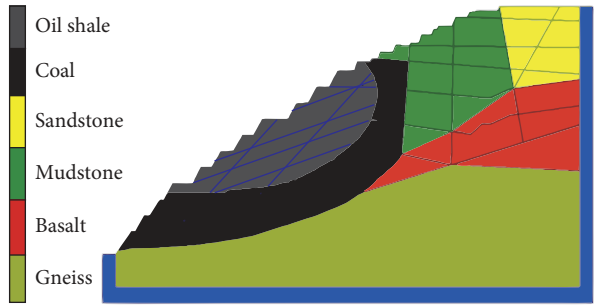

Figure 7: DDA model of the slope in the Fushun West Open-Pit Mine for numerical calculation and analysis.

Table 4: Mechanical parameters of the slope model.

Lithology	Density ($kg \cdot m^{-3}$)	E (GPa)	Cohesion (MPa)	Friction (°)
Oil shale	2100	16.5	3.5	26
Coal	1500	12.0	4.7	25
Sandstone	2300	15.2	20.0	19
Mudstone	2500	12.5	33.0	20
Basalt	2800	57.5	27.0	25
Gneiss	2800	38.2	32.0	29

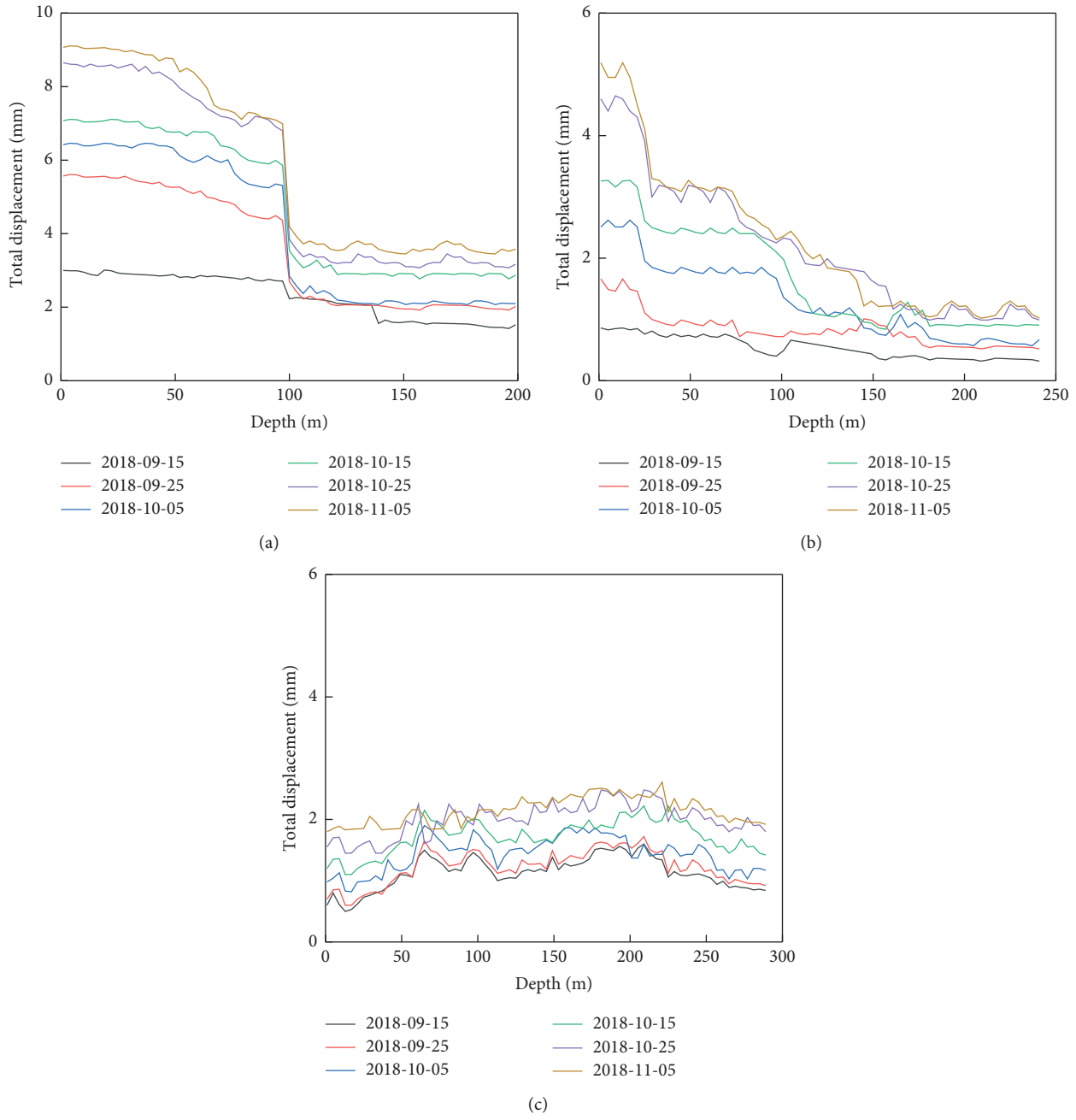

Figure 8: Cumulative displacements of the monitoring point in surveying the inclined hole: (a) surveying inclined hole 69002; (b) surveying inclined hole 55026; (c) surveying inclined hole 74003.

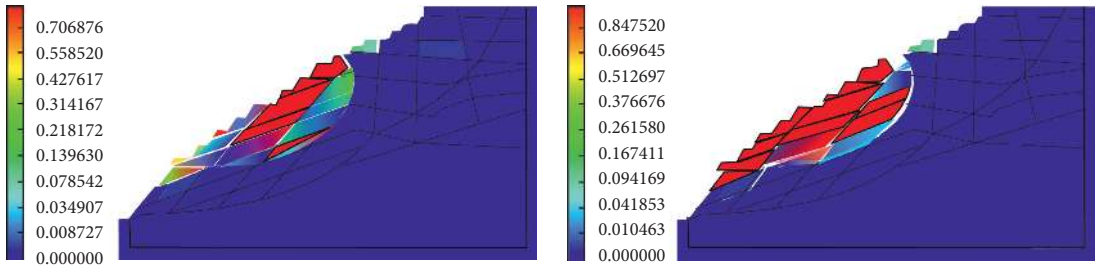

Figure 9: Continued.

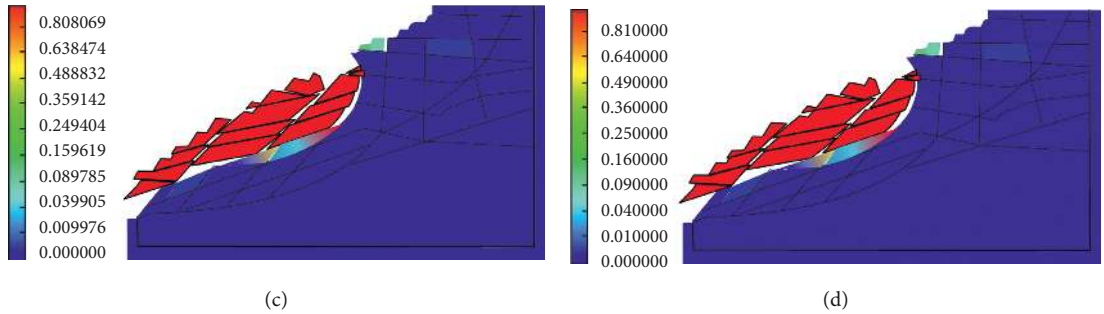

Figure 9: First failure process of the northern slope in the Fushun West Open-Pit Mine: (a) step 1.361×10^6; (b) step 1.363×10^6; (c) step 1.365×10^6; (d) step 1.367×10^6.

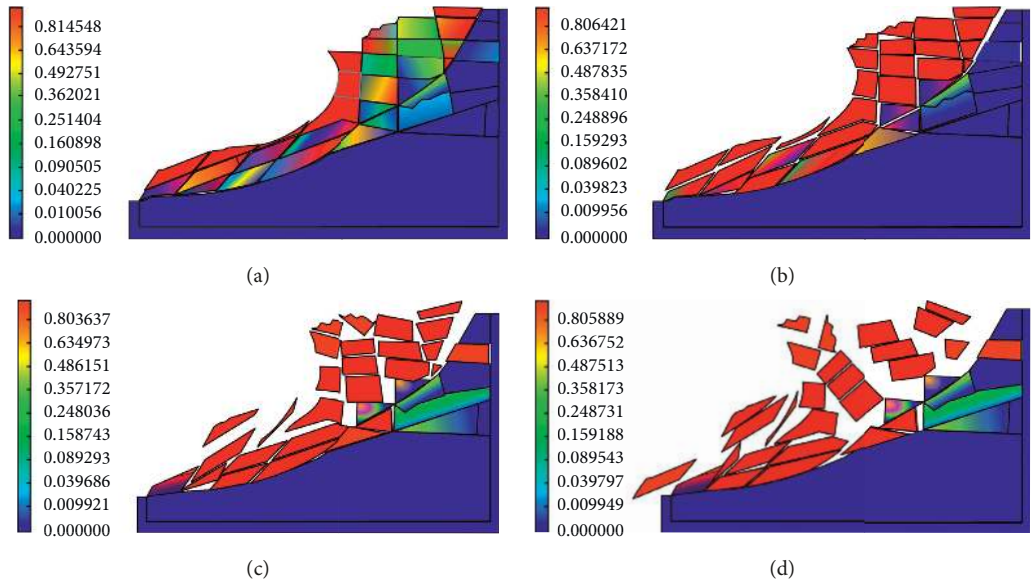

Figure 10: Second failure process of the northern slope in the Fushun West Open-Pit Mine: (a) step 1.892×10^6; (b) step 1.894×10^6; (c) step 1.896×10^6; (d) step 1.898×10^6.

this method will be improved to solve the problems of tunnel assessment and the failure mechanisms of different rocks [40–42].

6. Conclusions

This study aims to elucidate the problem of different degrees of damage along a rock mass structural plane and numerical model selection for analyzing slopes with multiple sliding surfaces. Furthermore, a series of numerical simulations and on-site monitoring data were used to study the mechanism controlling different degrees of damage along a rock mass structural plane. The following conclusions have been drawn from this study:

(1) A DSR-DDA method controlled by the displacement threshold is proposed. The basic process of calculating the safety factor of a slope with multiple sliding surfaces by the DSR-DDA method is provided, contributing a new method for slope-stability analysis.

(2) The feasibility and calculation accuracy of the DSR-DDA method are verified by the case of the classic slope slider. The displacement threshold is 1 mm, and the dynamic strength of the rock mass is reduced under different degrees of damage. Furthermore, the heterogeneity of the rock mass structural surface damage was analyzed.

(3) Based on the DSR-DDA method, the stability of multiple sliding surfaces of the northern slope of the Fushun West Open-Pit Mine was analyzed. The most dangerous slip surface and secondary slip surface position were determined, proving that the slope is prone to slipping. The results suggest that there is a requirement of dynamic change in the model for accurate slope surface stability analysis. The results indicate that the failure mode of the slope was traction sliding failure. The middle and lower oil shales play a key role in the stability of the slope. Therefore, the remaining oil shale cannot be continuously mined to avoid large-scale landslides and

landslides along the pit-city boundary in the upper part of the slope.

Data Availability

The data used to support the findings of this study are available from the corresponding author upon request.

Conflicts of Interest

The authors declare no conflicts of interest.

Authors' Contributions

Shuhong Wang and Chengjin Zhu contributed equally.

Acknowledgments

The authors gratefully acknowledge the financial support from the National Natural Science Foundation of China (Nos. 51474050 and U1602232), Fundamental Research Funds for the Central Universities (No. N17010829), Doctoral Scientific Research Foundation of Liaoning Province (Nos. 20170540304 and 20170520341), and Research and Development Project of Guizhou University of Engineering Science (Grant No: G2018016).

References

[1] C. Zhu, Z. Tao, Y. Shen, and S. Zhao, "V shaped gully method for controlling rockfall on high-steep slopes in China," *Bulletin of Engineering Geology and the Environment*, vol. 78, no. 4, pp. 2731–2747, 2019.

[2] Y. Li, S. Zhang, and X. Zhang, "Classification and fractal characteristics of coal rock fragments under uniaxial cyclic loading conditions," *Arabian Journal of Geosciences*, vol. 11, no. 9, p. 201, 2018.

[3] S. Zhang, Y. Li, B. Shen, X. Sun, and L. Gao, "Effective evaluation of pressure relief drilling for reducing rock bursts and its application in underground coal mines," *International Journal of Rock Mechanics and Mining Sciences*, vol. 114, pp. 7–16, 2019.

[4] Z. Qin, H. Fu, and X. Chen, "A study on altered granite meso-damage mechanisms due to water invasion-water loss cycles," *Environmental Earth Sciences*, vol. 78, p. 428, 2019.

[5] FQ. Ren, C. Zhu, and M. C. He, "Moment tensor analysis of acoustic emissions for cracking mechanisms during schist strain burst," *Rock Mechanics and Rock Engineering*, vol. 3, pp. 1–18, 2019.

[6] Z. Tao, Y. Wang, C. Zhu et al., "Mechanical evolution of constant resistance and large deformation anchor cables and their application in landslide monitoring," *Bulletin of Engineering Geology and the Environment*, vol. 78, no. 7, pp. 4787–4803, 2019.

[7] G. Shi, X. Yang, H. Yu, and C. Zhu, "Acoustic emission characteristics of creep fracture evolution in double-fracture fine sandstone under uniaxial compression," *Engineering Fracture Mechanics*, vol. 210, pp. 13–28, 2019.

[8] S. Wang and P. Ni, "Application of block theory modeling on spatial block topological identification to rock slope stability analysis," *International Journal of Computational Methods*, vol. 11, no. 1, pp. 903–914, 2014.

[9] N. R. Morgenstern and V. E. Price, "The analysis of the stability of general slip surfaces," *Géotechnique*, vol. 15, no. 1, pp. 79–93, 1965.

[10] Y. Zheng, C. Chen, T. Liu, H. Zhang, K. Xia, and F. Liu, "Study on the mechanisms of flexural toppling failure in anti-inclined rock slopes using numerical and limit equilibrium models," *Engineering Geology*, vol. 237, pp. 116–128, 2018.

[11] S.-H. Jiang, J. Huang, C. Yao, and J. Yang, "Quantitative risk assessment of slope failure in 2-d spatially variable soils by limit equilibrium method," *Applied Mathematical Modelling*, vol. 47, pp. 710–725, 2017.

[12] O. Simon, T. Franz, and F. S. Helmut, "Finite element analysis of slope stability problems using non-associated plasticity," *Journal of Rock Mechanics and Geotechnical Engineering*, vol. 10, no. 6, pp. 1091–1101, 2018.

[13] Y. Liu, W. Zhang, L. Zhang, Z. Zhu, J. Hu, and H. Wei, "Probabilistic stability analyses of undrained slopes by 3D random fields and finite element methods," *Geoscience Frontiers*, vol. 9, no. 6, pp. 1657–1664, 2018.

[14] L. Li, S. X. Liu, J. X. Li, and W. Jia, "Numerical simulation of oblique and multidirectional wave propagation and breaking on steep slope based on FEM model of Boussinesq equations," *Applied Mathematical Modelling*, vol. 71, pp. 632–655, 2019.

[15] J. M. Duncan, "State of the art: limit equilibrium and finite-element analysis of slopes. discussion and closure," *Journal of Geotechnical Engineering*, vol. 122, no. 7, pp. 577–596, 1996.

[16] M. Cala, J. Flisiak, and A. Tajdus, "Slope stability analysis with modified shear strength reduction technique," in *Proceedings of the Ninth International Symposium on Landslides: Evaluation and Stabilization*, Rio de Janeiro, Brazil, 2004.

[17] G.-H. Shi and R. E. Goodman, "Two dimensional discontinuous deformation analysis," *International Journal for Numerical and Analytical Methods in Geomechanics*, vol. 9, no. 6, pp. 541–556, 1985.

[18] M. Maclaughlin, N. Sitar, D. Doolin, and T. Abbot, "Investigation of slope-stability kinematics using discontinuous deformation analysis," *International Journal of Rock Mechanics and Mining Sciences*, vol. 38, no. 5, pp. 753–762, 2001.

[19] Y. H. Hatzor and A. Feintuch, "The validity of dynamic block displacement prediction using DDA," *International Journal of Rock Mechanics and Mining Sciences*, vol. 38, no. 4, pp. 599–606, 2001.

[20] S. A. R. Beyabanaki, B. Ferdosi, and S. Mohammadi, "Validation of dynamic block displacement analysis and modification of edge-to-edge contact constraints in 3-D DDA," *International Journal of Rock Mechanics and Mining Sciences*, vol. 46, no. 7, pp. 1223–1234, 2009.

[21] W. Jiang and H. Zheng, "An efficient remedy for the false volume expansion of DDA when simulating large rotation," *Computers and Geotechnics*, vol. 70, pp. 18–23, 2015.

[22] W. E. Morgan and M. M. Aral, "An implicitly coupled hydro-geomechanical model for hydraulic fracture simulation with the discontinuous deformation analysis," *International Journal of Rock Mechanics and Mining Sciences*, vol. 73, pp. 82–94, 2015.

[23] J.-H. Wu, "The elastic distortion problem with large rotation in discontinuous deformation analysis," *Computers and Geotechnics*, vol. 69, pp. 352–364, 2015.

[24] Y. Yu and J. Yin, "Some modifications to the process of discontinuous deformation analysis," *Journal of Rock Mechanics and Geotechnical Engineering*, vol. 7, no. 1, pp. 95–100, 2015.

[25] G. Yagoda-Biran and Y. H. Hatzor, "Benchmarking the numerical discontinuous deformation analysis method," *Computers and Geotechnics*, vol. 71, pp. 30–46, 2016.

[26] H. Zheng, P. Zhang, and X. Du, "Dual form of discontinuous deformation analysis," *Computer Methods in Applied Mechanics and Engineering*, vol. 305, pp. 196–216, 2016.
[27] G. Y. Fu, G. W. Ma, and X. L. Qu, "Boundary element based discontinuous deformation analysis," *International Journal for Numerical and Analytical Methods in Geomechanics*, vol. 41, no. 7, pp. 994–1015, 2017.
[28] H. Fan, H. Zheng, and J. Zhao, "Discontinuous deformation analysis based on strain-rotation decomposition," *International Journal of Rock Mechanics and Mining Sciences*, vol. 92, pp. 19–29, 2017.
[29] H. Fan, H. Zheng, and J. Wang, "A generalized contact potential and its application in discontinuous deformation analysis," *Computers and Geotechnics*, vol. 99, pp. 104–114, 2018.
[30] X. Fu, Q. Sheng, Y. Zhang, J. Chen, S. Zhang, and Z. Zhang, "Computation of the safety factor for slope stability using discontinuous deformation analysis and the vector sum method," *Computers and Geotechnics*, vol. 92, pp. 68–76, 2017.
[31] M. H. Shahami, A. Y. Bafghi, and M. F. Marji, "Investigating the effect of external forces on the displacement accuracy of discontinuous deformation analysis (DDA) method," *Computers and Geotechnics*, vol. 111, pp. 313–323, 2019.
[32] B. Gong, C. A. Tang, and S. Y. Wang, "Simulation of the nonlinear mechanical behaviors of jointed rock masses based on the improved discontinuous deformation and displacement method," *International Journal of Rock Mechanics and Mining Sciences*, vol. 122, 2019.
[33] K.-T. Chen and J.-H. Wu, "Simulating the failure process of the Xinmo Landslide using discontinuous deformation analysis," *Engineering Geology*, vol. 239, pp. 269–281, 2018.
[34] S. Fan, T. Li, X. Liu, L. Zhao, Z. Niu, and H. Qi, "A hybrid algorithm of partitioned finite element and interface element for dynamic contact problems with discontinuous deformation," *Computers and Geotechnics*, vol. 101, pp. 130–140, 2018.
[35] X. Liu and Z. Zhao, "Dynamic analysis with flat-top partition of unity-based discontinuous deformation analysis," *Computers and Geotechnics*, vol. 98, pp. 35–47, 2018.
[36] G. H. Shi, "Discontinuous deformation analysis: a new numerical model for the statics and dynamics of deformable block structures," *Engineering Computations*, vol. 9, no. 2, pp. 157–168, 1992.
[37] S. Wang, Z. Zhang, C. Wang, C. Zhu, and Y. Ren, "Multistep rocky slope stability analysis based on unmanned aerial vehicle photogrammetry," *Environmental Earth Sciences*, vol. 78, no. 8, pp. 260–275, 2019.
[38] Y. Tu, X. Liu, Z. Zhong, and Y. Li, "New criteria for defining slope failure using the strength reduction method," *Engineering Geology*, vol. 212, pp. 63–71, 2016.
[39] J. Song, Q. Fan, T. Feng, Z. Chen, J. Chen, and Y. Gao, "A multi-block sliding approach to calculate the permanent seismic displacement of slopes," *Engineering Geology*, vol. 255, pp. 48–58, 2019.
[40] J. Wang, S.-C. Li, L.-P. Li, P. Lin, Z.-H. Xu, and C.-L. Gao, "Attribute recognition model for risk assessment of water inrush," *Bulletin of Engineering Geology and the Environment*, vol. 78, no. 2, pp. 1057–1071, 2019.
[41] G. Feng, Y. Kang, Z.-D. Sun, X.-C. Wang, and Y.-Q. Hu, "Effects of supercritical CO2 adsorption on the mechanical characteristics and failure mechanisms of shale," *Energy*, vol. 173, pp. 870–882, 2019.
[42] W. Sun, H. Du, F. Zhou, and J. Shao, "Experimental study of crack propagation of rock-like specimens containing conjugate fractures," *Geomechanics and Engineering*, vol. 17, no. 4, pp. 323–331, 2019.